



Purification and characterization of the Lassa virus transmembrane domain

Patrick M. Keating, Hallie N. Pennington, Shane D. Collins, Jinwoo Lee *

Department of Chemistry and Biochemistry, University of Maryland College Park, College Park, MD, 20742, USA

ARTICLE INFO

Keywords:

Transmembrane domain
Sodium trichloroacetate
Detergent screening
Lassa virus
Glycoprotein
LMPG

ABSTRACT

Lassa virus (LASV) is the most prevalent arenavirus afflicting humans and has high potential to become a threat to global public health. The transmembrane domain (TM) of the LASV glycoprotein complex forms critical interactions with the LASV stable signal peptide that are important for the maturation and fusion activity of the virus. A further study of the structure-based molecular mechanisms is required to understand the role of the TM in the lifecycle of LASV in greater detail. However, it is challenging to obtain the TM in high quantity and purity due to its hydrophobic nature which results in solubility issues that makes it prone to aggregation in typical buffer systems. Here, we designed a purification and detergent screen protocol for the highly insoluble TM to enhance the yield and purity for structural studies. Based on the detergents tested, the TM had the highest incorporation in LMPG. Circular dichroism (CD) and nuclear magnetic resonance (NMR) spectroscopy were utilized to confirm the best detergent system for structural studies. Through CD spectroscopy, we were able to characterize the secondary structure of the TM as largely alpha-helical, while NMR spectroscopy showed a well-structured and stable TM in LMPG. From these results, LMPG was determined to be the optimal detergent for further structural studies.

1. Introduction

Infection with Lassa virus (LASV), an arenavirus endemic to West Africa, results in Lassa fever, a viral hemorrhagic fever with high morbidity and mortality [1,2]. LASV is spread to humans via direct contact with infected *Mastomys natalensis* excrement, a rodent serving as the natural reservoir of LASV [3]. Furthermore, there is evidence of the virus being transmitted between humans through contact with bodily fluids, even after recovery from the infection [4]. LASV is estimated to infect 300,000–500,000 people and cause 5000 deaths annually in West Africa [5]. Currently, there are no options for the explicit treatment of LASV infection. The only alternative is off-label usage of ribavirin, an antiviral drug used to treat a wide variety of viral infections [6]. However, ribavirin is only effective if administered in the early stages of infection, has an unknown mechanism of action against LASV, and causes severe side effects [7]. With no approved therapeutics or vaccines, LASV poses a significant public health risk should it spread outside West Africa. In fact, the World Health Organization (WHO) lists Lassa fever as one of the top infectious diseases requiring prioritized research and development [8]. There have already been isolated cases of LASV infection outside of West Africa in Europe and the United States [9,10].

The glycoprotein complex (GPC) is the sole component on the LASV

surface and is responsible for viral entry into the cell (Fig. 1A). The GPC consists of a trimer of heterotrimers containing glycoprotein 1 (GP1), glycoprotein 2 (GP2), and the stable signal peptide (SSP). GP1 is responsible for binding to the cellular receptors while GP2 is responsible for facilitating membrane fusion to deliver the genetic information into the cells. The SSP resides next to the transmembrane domain (TM) of GP2 in the viral membrane and plays various roles in the viral lifecycle, including the maturation of the GPC and membrane fusion [11,12]. Not only is the TM important for LASV, but other viruses have been shown to have important roles for their transmembrane domains in membrane fusion. The TM of the Ebola and Influenza virus glycoproteins form an interaction with their respective fusion domains of the glycoproteins, enhancing membrane fusion [13,14]. Furthermore, the structure of the TM can be impacted by the viral membrane lipids, which can also influence membrane fusion. In particular, cholesterol has been shown to interact with the TM of HIV, Ebola and Influenza and impacted viral membrane fusion in all cases [15–17]. In HIV, a broadly neutralizing antibody LN01 targets the TM and membrane-proximal external region (MPER) domain of gp41, suggesting that the TM serves as a valuable therapeutic target for viral infection [18]. In LASV, previous cell-based studies with the small molecule inhibitors ST-161, derivatives of ST-161, and the antifungal isavuconazole were all shown to disrupt the interaction between the TM and the first transmembrane helix of the SSP,

* Corresponding author.

E-mail address: jinwoo@umd.edu (J. Lee).

Abbreviations	
DPC	dodecylphosphocholine
LMPG	1-myristoyl-2-hydroxy-sn-glycero-3-phospho-(1'-rac-glycerol)
CHAPS	3-[(3-cholamidopropyl)-dimethylammonio]-1-propane sulfonate
β -OG	n-octyl- β -D-glucopyranoside
DHPC	1,2-dihexanoyl-sn-glycero-3-phosphocholine
LDAO	N-N,Dimethyl-1-dodecylamine N-oxide
TCA	sodium trichloroacetate
BME	β -mercaptoethanol
LASV	Lassa virus
TM	transmembrane domain
SSP	stable signal peptide
GP2	glycoprotein 2
GPC	glycoprotein complex

present a purification protocol for the structural characterization of the LASV TM (residues 424–461). We expressed and purified the TM, which is prone to have non-specific interactions that result in a high tendency to aggregate, making it difficult to purify. To overcome these challenges, we utilize the aggregating tendency of the TM to our advantage. We intentionally aggregate the TM and remove all unwanted proteins, then break apart the TM aggregates with the strong denaturant sodium trichloroacetate (TCA) to isolate the pure TM. Once the pure TM was isolated in TCA, we determined which detergents would be suitable for structural studies by exchanging the TM into various detergent systems using a desalting column. Analysis by SDS-PAGE gel of this desalting column method revealed that 1-myristoyl-2-hydroxy-sn-glycero-3-phospho-(1'-rac-glycerol) (LMPG) and dodecylphosphocholine (DPC) were the most suitable detergents for the LASV TM. We then turned to CD and NMR spectroscopy to characterize the structure and stability of the TM in the detergents, respectively. CD spectroscopy revealed that the TM contains alpha-helical character in both detergent systems, with increased helicity noted in LMPG. However, NMR spectroscopy clearly illustrated that the TM was more stable in the LMPG system than the DPC system, indicating that LMPG is the most optimal detergent for further structural studies.

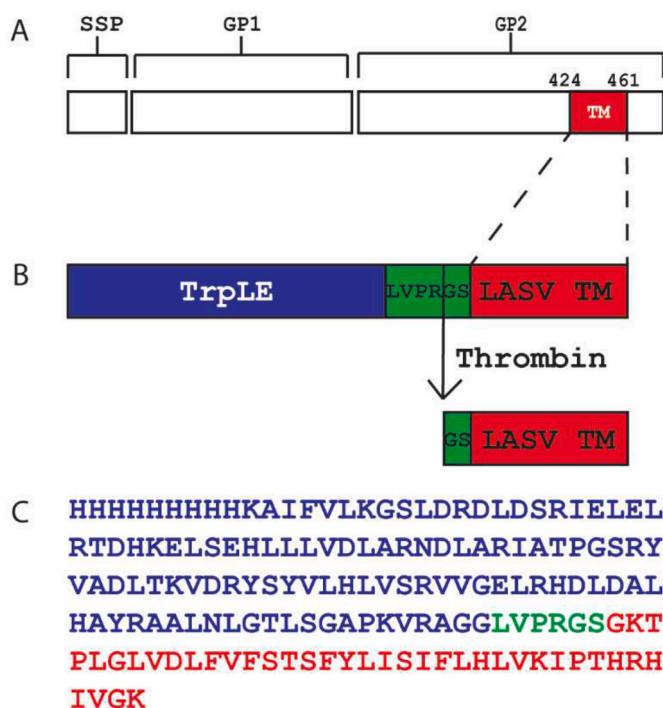


Fig. 1. LASV GPC and Construct Design. A) Schematic of the proteins in the LASV GPC with the TM highlighted in red. SSP – stable signal peptide; GP1 – glycoprotein 1; GP2 – glycoprotein 2. B) Schematic of TM construct before and after thrombin cleavage. Two artificial amino acids are added to the N-terminus of TM due to thrombin cleaving between R and G. C) Sequence of TrpLE_TM construct with the TrpLE in blue, thrombin cleavage site in green and TM sequence in red.

resulting in the hindrance of membrane fusion [19–21]. This illustrates the importance of the TM of LASV in membrane fusion; however, we are still in need of structural information to understand the underlying mechanism of LASV TM during the fusion process.

The lack of knowledge surrounding the LASV TM can be attributed to the difficulty of purifying membrane proteins. Although there are various methods for purifying membrane proteins, including methods successfully applied to other viral transmembrane domains, they are not without their challenges, especially for proteins that are prone to aggregate in solution, like the highly insoluble LASV TM. Here, we

2. Materials and Methods

2.1. Reagents

Dodecylphosphocholine (DPC) (CA# F308), 3-[(3-cholamidopropyl)-dimethylammonio]-1-propane sulfonate (CHAPS) (CA# C316), and n-octyl- β -D-glucopyranoside (β -OG) (CA# O311) were purchased from Anatrace. LMPG (CA# 858120) and 1,2-dihexanoyl-sn-glycero-3-phosphocholine (DHPC) (CA# 850305) were purchased from Avanti Polar Lipids. Empigen BB™ (CA# 30326-250 ML) was purchased from Millipore Sigma. N-N,Dimethyl-1-dodecylamine N-oxide (LDAO) (CA# 1643-20-5) and sodium trichloroacetate (CA# AAA170040I) were purchased from Fisher Scientific. All lipids and detergents were stored at -20°C and allowed to warm to room temperature prior to use.

2.2. Construct Design and cloning

The LASV TM was generated from a LASV glycoprotein complex (GPC) plasmid generously provided by the Judith M. White lab (University of Virginia). The constructs were inserted into the pET24a vector containing an N-terminal Hisx9 tag, Trp leading sequence (TrpLE), thrombin cleavage site, and kanamycin resistance gene (Fig. 1B and C). The TrpLE sequence was chosen for these experiments as it directs the protein to inclusion bodies, improving yield and preventing harm to the cells during expression [22,23].

For insertion of the TM gene sequence into the pET24a vector, *Bam*H1 and *Eco*R1 restriction sites were added to the 5' and 3' ends of the gene, respectively. Both the 5' and 3' ends contained additional base pairs for efficient digestion. The DNA oligos (Table S1) were synthesized (IDT, Inc, Coralville, IA, USA) and added to a reaction mixture containing the following components in a 50 μL reaction scale: forward and reverse oligo (200 nM final concentration), template DNA (2 ng/ μL), dNTPs (200 nM), 5X HF Buffer (New England Biolabs, Ipswich, MA, USA), ultrapure water, and 1 μL Phusion HF Polymerase (New England Biolabs, Ipswich, MA, USA). The PCR amplified gene was run on a 1% agarose gel stained with Apex Safe DNA Gel Stain (Genesee Scientific) and extracted. Extracted PCR product and pET24a vector were purified and digested with 1 μL each of both *Bam*H1 and *Eco*R1 (New England Biolabs) overnight at room temperature. Ligation of the pET24a vector and TM gene sequence were carried out using 1 μL DNA Ligase (New England Biolabs) overnight at room temperature. After ligation, the plasmid was transformed into DH5 α *E. coli* cells (New England Biolabs) and grown on a Luria-Bertani (LB) plate containing 50 $\mu\text{g}/\text{mL}$ kanamycin overnight at 37°C . Colonies were sequenced (ACGT, Inc.,

Germantown, MD, USA) to confirm the insertion of the protein sequence (Table S2). For protein expression, the plasmid containing the correct sequence was transformed into BL21 (DE3) pLysS *E. coli* cells (ThermoFisher Scientific) and grown on LB plates containing 50 µg/mL kanamycin and 34 µg/mL chloramphenicol overnight at 37 °C. Colonies from the transformation were used to perform test expressions in a 1 mL scale and a glycerol stock was prepared for future use. For insertion of the GP2 gene sequence, restriction enzymes were chosen based on its sequence and preparation of the plasmids was performed using the above protocol.

2.3. Expression and purification

A general scheme for the purification method is shown in Fig. 2A. Cells from a glycerol stock were grown in a 5 mL LB culture containing 50 µg/mL kanamycin and 34 µg/mL chloramphenicol overnight at 37 °C while shaking at 225 rpm. The 5 mL overnight culture was used to inoculate 1L of LB media containing 50 µg/mL kanamycin and 34 µg/mL chloramphenicol. The cells were grown at 37 °C while shaking at 225 rpm until an optical density at 600 nm (OD_{600}) of 0.6–0.8 was reached. The cells were then induced with a final concentration of 1 mM Isopropyl β-D-1-thiogalactopyranoside (IPTG). The cells were grown for an additional 4 h at 37 °C after induction, then harvested at 4,000×g for 45 min at 4 °C. The cell pellet was used immediately or stored at –80 °C until needed.

After harvesting, 1L of cells were resuspended in 120 mL sucrose buffer (20% sucrose (w/v), 300 mM NaCl, 20 mM tris, 10 mM BME, pH 8.0). The sample was then sonicated on ice for 5 min at a 40% duty cycle with a cycle of 1 s on/off. After sonication, the solution was centrifuged at 40,000×g at 4 °C for 1 h to isolate the inclusion bodies. The supernatant was discarded, as the target protein was left in the resulting pellet. Following this, the target protein was solubilized in 100 mL sodium trichloroacetate (TCA) buffer (4.5 M TCA, 300 mM NaCl, 20 mM tris, 10 mM BME, 10 mM imidazole, pH 8.0), sonicated with the same parameters as mentioned above, and centrifuged at 40,000×g at 20 °C for 1 h. The supernatant was then incubated overnight with approximately 3 mL Ni-NTA resin (Qiagen) at 20°C while shaking at 100 rpm.

Following incubation, the flowthrough was collected, and the resin was washed with a gradient in a stepwise fashion with 45 mL per step. The TCA concentration was decreased from 4.5 M to 0 M in 1 M increments while all other buffer components were kept the same. This

slowly removes the denaturing TCA, allowing the protein to refold gradually. After removing all the TCA from the resin, the resin was subsequently equilibrated with 15 mL cleavage buffer (0.1% DPC (w/v), 100 mM NaCl, 20 mM tris, 2.5 mM $CaCl_2$, pH 8.5). Once equilibrated, 50 µL of 5 mg/mL thrombin (BioPharm Laboratories) was added directly to the resin along with 15 mL of the cleavage buffer. The cleavage reaction proceeded overnight at room temperature while shaking at 100 rpm.

After cleavage, the flowthrough was collected. The resin was subsequently washed with 100 mL urea buffer (8 M urea, 20 mM tris, 300 mM NaCl, pH 8.0) containing 100 mM imidazole to remove the tag and other unwanted proteins followed by an additional 50 mL of tris buffer (20 mM tris, 300 mM NaCl, pH 8.0) to remove residual urea and imidazole. Finally, the resin was washed twice with 10 mL TCA buffer without BME or imidazole to elute the TM. The two TCA buffer washes containing the TM were combined and concentrated to 500 µL using an Amicon™ Ultra-15 3K MWCO spin concentrator for detergent screening. The TM was then buffer exchanged into a detergent buffer (100 mM detergent, 100 mM NaCl, 25 mM Na_2HPO_4 , pH 7.0) using a PD Mini-Trap™ G-25 desalting column (Cytiva), following the manufacturer's spin protocol. The same amount of detergent was also added to the concentrated sample prior to loading on the desalting column. To purify further the TM, size exclusion chromatography (SEC) was performed using an AKTA Pure™ FPLC (GE) with a Superdex™ 200 Increase 10/300 GL column (Cytiva). The column was pre-equilibrated with two column volumes of 25 mM Na_2HPO_4 , 100 mM NaCl, 2 mM LMPG, pH 7.0 and fractionated into 0.5 mL volumes. The GP2 purification followed a similar method with slight modifications. A detailed protocol can be found in the supplemental.

2.4. SDS-PAGE

Samples were prepared by the addition of 4X SDS loading buffer (200 mM Tris-HCl pH 6.8, 8% sodium dodecyl sulfate, 40% glycerol, 0.4% Bromophenol Blue, 572 mM BME) to a final concentration of 1X. Due to the viscosity of the TCA buffer, samples containing TCA were 10-fold diluted using 1X SDS loading buffer. 10 µL of each sample was loaded onto Tris-Tricine SDS-PAGE gels produced in the lab and run for 25 min at 200V. Samples containing guanidinium were first precipitated using a methanol-chloroform extraction, and then the protein pellet was solubilized in 1X SDS loading buffer [24].

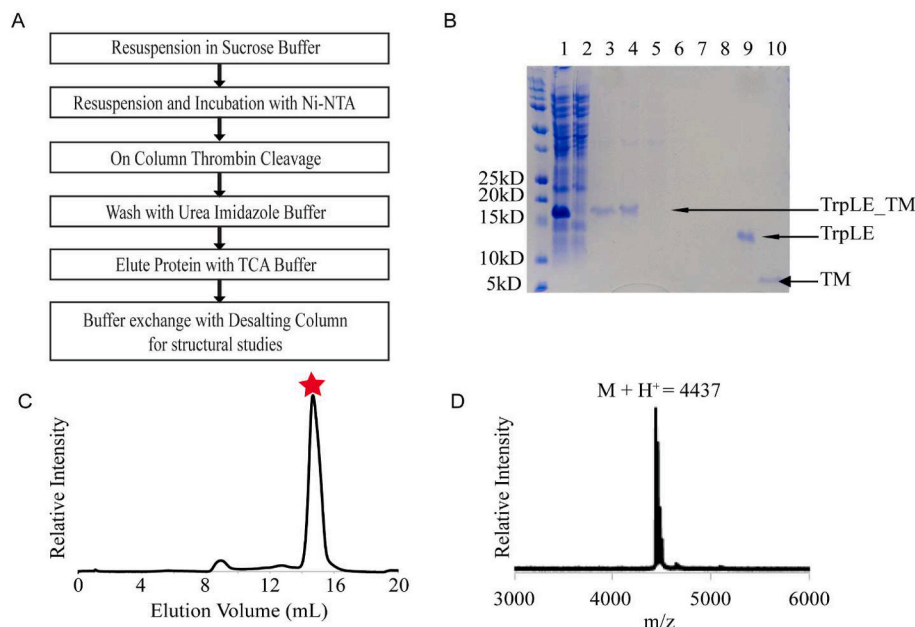


Fig. 2. Purification of the LASV TM. A) Flow chart illustrating the steps in the purification protocol. B) Tris-Tricine SDS-PAGE gel of the LASV TM purification samples. Lane 1, sucrose buffer pre centrifugation; lane 2, sucrose buffer post centrifugation; lane 3, TCA buffer pre centrifugation; lane 4, TCA buffer post centrifugation; lane 5, flowthrough from Ni-NTA incubation; lane 6, 4.5 M TCA buffer wash; lane 7, flowthrough from on-column thrombin cleavage; lane 8, 8 M urea buffer wash after cleavage; lane 9, 8 M urea buffer with 100 mM Imidazole wash after cleavage; lane 10, TM elution in TCA buffer. C) Size exclusion chromatography trace of purified LASV TM in 2 mM LMPG, 25 mM Na_2HPO_4 , 100 mM NaCl, pH 7.0. The red star denotes the LASV TM peak at an elution volume of 14.7 mL. D) MALDI-TOF mass spectrum of the LASV TM from the SEC confirms the molecular weight of the TM. The expected monoisotopic molecular weight is 4436 Da, observed is 4437 Da.

2.5. MALDI-TOF mass spectrometry

The identity of the isolated LASV TM was confirmed by matrix-assisted laser desorption ionization-time of flight (MALDI-TOF) mass spectrometry. 1.0 μ L of TM from the corresponding SEC fractions was combined with 1.5 μ L sinapinic acid matrix that was at a concentration of 10 mg/mL. Measurements were performed on a Bruker AutoflexTM Speed instrument using a linear polarized detection method with a range of 2000–16000 Da.

2.6. CD spectroscopy

CD measurements were performed on a Jasco J-810 spectrophotometer with a 0.2 cm quartz cuvette with a TM concentration of 15 μ M in 2.5 mM Na₂HPO₄, 10 mM NaCl, 10 mM LMPG, pH 7.0 at 37°C. Measurements were also collected in 2.5 mM Na₂HPO₄, 10 mM NaCl, 10 mM DPC, pH 7.0 at a TM concentration of 4 μ M. Spectra were obtained in triplicate from 260 nm to 190 nm with a step size of 1 nm at 50 nm/min. Measurements were taken for the buffer alone and subtracted from each sample using the provided software. Data analysis was performed using the CDSSTR method with set 7 as the reference in the DichroWeb server [25–29].

2.7. NMR spectroscopy

To label the TM with the ¹⁵N isotope, cells were grown in 1L M9 minimal media, containing 6.5 g/L Na₂HPO₄, 3.0 g/L KH₂PO₄, 0.5 g/L NaCl, 1.0 g/L ¹⁵NH₄Cl, 10 g/L glucose, 1 mM MgSO₄, 0.1 mM CaCl₂, trace amounts of thiamine and biotin, 50 μ g/mL kanamycin, and 34 μ g/mL chloramphenicol. Cells were grown until an OD₆₀₀ of 0.6–0.8 was reached. The cells were then induced with a final concentration of 1 mM IPTG for 18–20 h at 25°C before they were harvested at 4,000 \times g for 45 min at 4°C. Samples were purified as mentioned above and prepared in 25 mM Na₂HPO₄, 100 mM NaCl, pH 7.0, and either 100 mM LMPG or 120 mM DPC with 10% D₂O at a TM concentration of at least 0.25 mM ¹H–¹⁵N TROSY HSQC experiments were performed on a Bruker Ascend 800 MHz spectrometer equipped with a CPQCI cryoprobe at 37°C. Data were processed using NMRPipe and the spectrum and analysis were generated using NMRFAM-Sparky via NMRbox [30–32].

3. Results and discussion

3.1. Purification of the Lassa virus transmembrane domain

The hydrophobic LASV TM was expressed and purified as described in the Materials and Methods. The first step involved the removal of unwanted soluble proteins by resuspending the cell pellet in the sucrose buffer, which was followed by sonication and centrifugation. As we expected, the full-length TM (TrpLE_{TM}) was insoluble in the sucrose buffer and migrated to the pellet during centrifugation, signified by the absence of a TrpLE_{TM} band in the pre and post centrifugation sample on the SDS-PAGE gel (Fig. 2B, lanes 1 and 2). After removing the soluble proteins, TCA buffer was utilized to solubilize the TrpLE_{TM}. TCA is a strong denaturant that is more effective than urea and guanidinium, and has been used when purifying proteins previously [33,34]. We witnessed no significant pellet after centrifugation, indicating that TCA was able to solubilize all of the protein. The presence of the TrpLE_{TM} in the supernatant before and after centrifugation was also confirmed by SDS-PAGE gel (Fig. 2B, lanes 3 and 4). Once the TrpLE_{TM} was solubilized, the supernatant was incubated with Ni-NTA resin to bind the protein via the His-tag. We observed that the TrpLE_{TM} was not present in the flowthrough after incubation, indicating complete binding of the target protein (Fig. 2B, lane 5). This indicates that TCA is efficient at solubilizing the highly aggregating TrpLE_{TM}, allowing the His-tag to bind to the Ni-NTA resin.

To liberate the TM from the TrpLE tag, we employed the on-column

cleavage method using thrombin. However, the denaturant had to be removed to achieve efficient thrombin cleavage. Thus, a gradient wash of the Ni-NTA resin was executed to gently remove all the TCA and switch to the cleavage buffer (Fig. 2B, lane 6). This helped with the folding and transfer of the TrpLE_{TM} to a buffer that is compatible with thrombin to achieve efficient cleavage. Most membrane purification protocols involve cleavage require an appropriate detergent. Typically, detergents are optimized to collect the target protein in the flowthrough after cleavage as it is no longer associated with the His-tag and, hence, is liberated from the resin [13]. However, the LASV TM was not present in the flowthrough after cleavage and remained associated with the column (Fig. 2B, lane 7). This result was unexpected since the cleavage buffer contained a detergent intended to keep the membrane protein soluble during cleavage. This is thought to be due to non-specific interactions with either the resin or the protein itself that occurred after thrombin cleavage, resulting in aggregation and preventing elution of the TM in the cleavage flowthrough. Typically, to circumvent this problem, two approaches are taken. First, imidazole can be added to the buffer to prevent non-specific interactions of the protein with the Ni-NTA resin. However, we did not observe the target band even after introducing a high concentration of imidazole to the column (Fig. 2B, lane 9). Thus, we concluded that the binding of the TM to the resin was due to aggregation, not non-specific interactions with the resin. The second method is to switch the detergent in the cleavage buffer to a stronger detergent to prevent aggregation. However, there are few choices of detergents stronger than DPC that are used in structural studies and allow for efficient thrombin cleavage. Therefore, there was no simple way for us to solve the issue. Instead, to circumvent the problem, we utilized this strong aggregating property of the TM as a unique opportunity to simplify and enhance the purification by removing all proteins from the column after cleavage, then liberating the pure TM from the column using TCA.

We tested different denaturants to break apart the aggregates in an attempt to elute the TM from the resin successfully. We first used a urea buffer and found that it was unable to elute the TM from the resin (Fig. 2B, lane 8), suggesting that the interactions forming the aggregates were strong and could not be broken apart easily with just urea. We next tested the 4.5 M TCA buffer, which is a stronger denaturant than the urea buffer [33]. Interestingly, the TM was liberated from the Ni-NTA resin when the TCA buffer was applied (Fig. 2B, lane 10). Since a strong denaturant like TCA is required to break the aggregates and release the TM from the Ni-NTA column, we can utilize a urea and imidazole wash to further purify the TM before its elution. Furthermore, this method provides a unique way to purify a protein with a propensity to aggregate, resulting in the target protein in the TCA buffer at a high level of purity (Fig. 2B, lane 10).

Our purification method takes advantage of the hydrophobic property of a membrane protein that is prone to aggregate to obtain a high-purity sample. As such, we believe that this protocol can be expanded to other membrane proteins. To expand this protocol, it is essential that the protein becomes aggregated following cleavage. To ensure the TM aggregated, we removed the detergent from the cleavage buffer and tested the enzymatic cleavage. When we compared the results involving cleavage with or without detergent in the cleavage buffer, both showed successful cleavage and isolated TM in the TCA buffer (Fig. S1). The cleavage without detergent in the buffer ensured that the TM was aggregated and the cleavage event was not disrupted by the aggregation after cleavage. We believe the application of this protocol is versatile and can be applied to other membrane proteins that are difficult to purify.

We demonstrated the possibility for expansion of this protocol by applying the method to a longer construct of the GP2 (residues 260–461). The LASV GP2 construct contains multiple hydrophobic domains primarily in its N-terminal fusion domain and the TM, which adds more complexity to its purification [11]. We were able to successfully expand our purification protocol by applying the method to the GP2

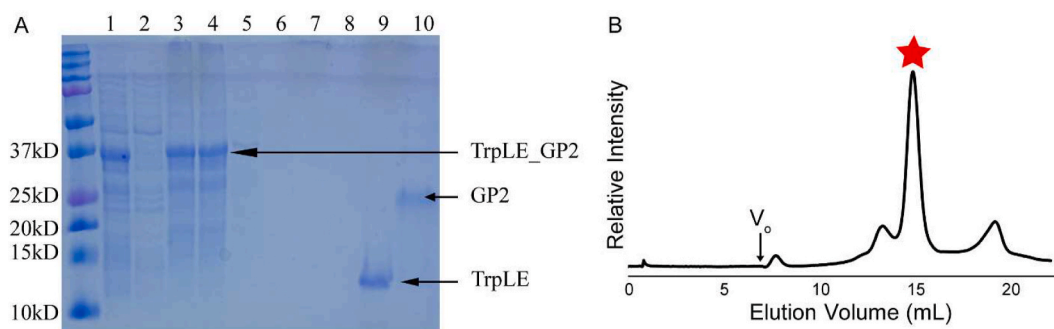


Fig. 3. GP2 Purification. A) Tris-Tricine SDS-PAGE gel of GP2 purification samples. Lane 1, sucrose buffer pre centrifugation; lane 2, sucrose buffer post centrifugation; lane 3, resuspension buffer pre centrifugation; lane 4, resuspension buffer post centrifugation; lane 5, flowthrough from Ni-NTA incubation; lane 6, 6 M guanidine buffer wash; lane 7, flowthrough from on-column thrombin cleavage; lane 8, 8 M urea buffer wash after cleavage; lane 9, 8 M urea buffer with 100 mM Imidazole wash after cleavage; lane 10, GP2 elution in TCA buffer. B) SEC trace of the GP2. The red star denotes the GP2 at an elution volume of ~ 15 mL.

(Fig. 3A). The GP2 was also cleaved with and without detergent in the cleavage buffer and aggregated on the column (Fig. S2). We used the same TCA buffer to elute the GP2 from the column with high purity and polished the sample with size exclusion chromatography (Fig. 3B). Taking advantage of the natural hydrophobic properties of the membrane proteins, we obtained high purity GP2 suggesting the protocol can be expanded to other membrane proteins.

3.2. Characterization of the TM

Following effective isolation of the TM, we aimed to determine the optimal detergent for the TM for the structural studies via a desalting column. The advantage of this protocol is that the desalting column can easily remove the TCA, which makes exchanging the TM to a detergent system relatively quick and straightforward. Furthermore, the protein sample can be divided and used to test several different detergents simultaneously since this method does not require a high protein concentration for SDS-PAGE gel analysis. Using the desalting column, we buffer exchanged the TM from TCA buffer into different detergent buffers containing 100 mM of either LMPG, DPC, β -OG, CHAPS, or DHPC, allowing the TM to be incorporated into detergent micelles (Fig. 4A). These detergents were chosen as they are commonly used for biochemical or biophysical characterization of membrane proteins, especially in solution NMR [35,36]. After incorporation, we centrifuged the samples to remove any insoluble portions and analyzed the supernatant on a Tris-Tricine SDS-PAGE gel. This centrifugation removed any TM that was not folded properly into a native conformation and formed aggregates in the detergent. The gel revealed that the LMPG supernatant had the highest TM concentration compared to the other detergents

(Fig. 4B), with DPC containing the second highest amount, suggesting that the TM is most soluble in LMPG buffer. While the zwitterionic DPC, DHPC, and CHAPS as well as the uncharged β -OG were able to solubilize some of the TM, there was significantly less protein in the supernatant in comparison to the anionic LMPG. The charged state of the detergent leads to an increase in strength, which is evidently needed for the TM to be soluble in solution, likely preventing the tendency for aggregation. Although we focused on detergent systems, this method could potentially be expanded to other membrane mimics as well.

Since LMPG was the best at solubilizing the TM, we used LMPG to further polish the TM with SEC, which showed pure sample quality (Fig. 2C). Furthermore, we performed MALDI-TOF mass spectrometry and confirmed the identity of the TM (Fig. 2D). The expected monoisotopic mass of the TM is 4436Da and we observed 4437Da, indicative of an $M+H^+$ ion.

Once we performed the detergent screen and confirmed the mass of the TM, we used CD spectroscopy to analyze the global secondary structure of the TM. The CD spectra of the TM in both LMPG and DPC were performed at 37°C to give a more physiologically relevant environment and demonstrated alpha-helical characteristics with notable minima at 208 and 222 nm (Fig. 5). The alpha-helical character aligns well with other viral transmembrane domains such as HIV, Influenza and SARS-CoV-2, which also show alpha-helical structure in their transmembrane domains [37–39]. This result also corroborates the predictions that this region contained an alpha helix [19,20]. These characteristics indicated that the TCA was successfully removed from the solution with the desalting column. If there were any TCA present, we would expect to see a spectrum indicating a more random coil as the folding would be disrupted.

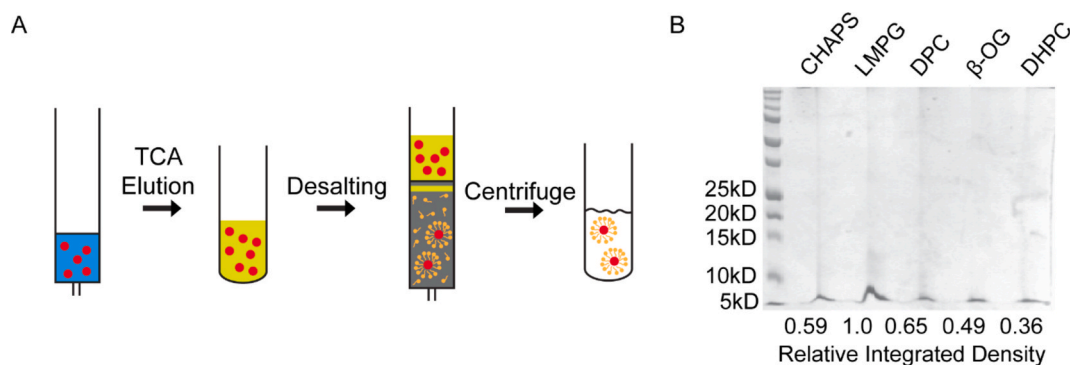


Fig. 4. Detergent screen of the LASV TM. (A) Schematic of detergent screen. The TM (red dots), which was aggregated in the Ni-NTA resin (blue), was eluted using TCA buffer (yellow-green). The TM was then buffer exchanged from TCA buffer to detergent buffer (25 mM Na_2HPO_4 , 100 mM NaCl, pH 7.0, 100 mM detergent) using a desalting column (grey). Following buffer exchange, samples were centrifuged to collect insoluble portion and the supernatants were analyzed by Tris-Tricine SDS-PAGE gel (B). Density was determined using ImageJ software by taking the ratio of the integrated density of each band relative to the LMPG band [42]. LMPG was the densest and has the most protein compared to the other detergents.

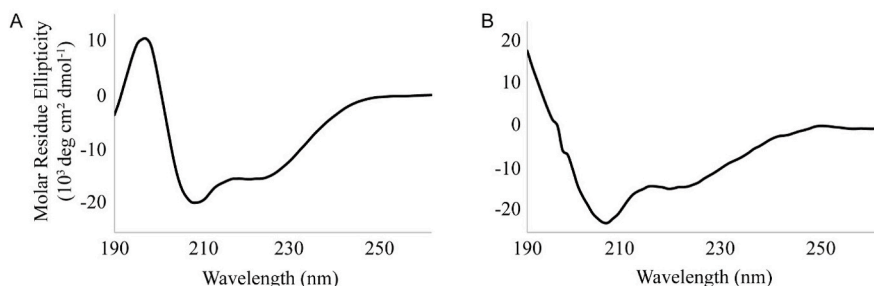


Fig. 5. CD Spectra of TM in Detergent. CD spectra of TM in LMPG (A) and DPC (B) showing alpha-helical character.

Further analysis of the secondary structure was performed using DichroWeb. We chose to use the CDSSTR method for analysis as it gave the lowest NRMSD among all the methods tested [26,40]. The analysis revealed that the TM had 59% helicity in LMPG (32% regular helix and 27% distorted helix) compared to a total of 40% helicity in DPC (22% and 18%, respectively), where distorted refers to the terminal residues in the helix having distorted secondary structure (i.e. bends, end fraying, etc.) [41]. This content corresponds to a 36 Å helix containing 24 amino acids in LMPG versus a 24 Å helix with 16 amino acids in DPC. The 19% higher alpha helical character in LMPG could be due to the differences in the detergents, such as charge and chain length, that influence the protein's stability. The anionic head group of LMPG may preferentially interact with the TM, stabilizing it and allowing for the formation of a longer helix, whereas the zwitterionic DPC does not have the same preference due to its weaker charged state, therefore unable to form a longer helix. Furthermore, the 14-carbon chain LMPG may work in tandem with its anionic head group to further stabilize the longer helix in comparison to the 12-carbon chain in DPC. When considering the other detergents tested than LMPG in the detergent screen, each had both a zwitterionic or non-ionic head group and shorter carbon chain. The combination of the anionic head group and longer carbon chain of LMPG appear to contribute to the stabilization the TM, leading to more helical content.

We performed NMR spectroscopy to further investigate the folding and quality of the TM in LMPG and DPC micelles. A ^1H - ^{15}N TROSY-HSQC revealed well-dispersed peaks in both LMPG and DPC, indicating that the TM was well structured (Fig. 6). However, the DPC spectrum had significantly fewer peaks and poorer resolution than LMPG. There are 38 expected peaks in the TM, due to 2 proline residues in the sequence, and 34 were observed in LMPG whereas only 19 peaks were observed in DPC. Moreover, all the peaks observed in the LMPG spectrum were sharper compared to the peaks in the DPC spectrum

Table 1

LASV TM peak characteristics in detergent micelles.

Detergent	Peak Height	Signal/Noise	Peak Volume (ga)	^1H Linewidth (Hz)	^{15}N Linewidth (Hz)
LMPG	$3.1 \pm 1.3 (10^7)$	153.3 ± 64.6	$3.6 \pm 1.6 (10^8)$	41.6 ± 11.7	28.9 ± 6.3
DPC	$6.3 \pm 1.7 (10^5)$	15.2 ± 4.2	$3.2 \pm 5.7 (10^7)$	87.6 ± 54.9	49.4 ± 55.0

Comparison of the average values of different parameters for each peak detected in the ^1H - ^{15}N TROSY-HSQC for the TM in 25 mM Na_2HPO_4 , 100 mM NaCl, pH 7.0 and either 100 mM LMPG or 120 mM DPC. Values calculated using NMRFAM-Sparky.

(Table 1). The peak height and peak-volume were significantly larger in LMPG ($3.1e7 \pm 1.3e7$ and $3.6e8 \pm 1.6e8$ ga, respectively) compared to DPC ($6.3e5 \pm 1.5e5$ and $3.2e7 \pm 5.7e7$ ga, respectively), indicating better sharpness in LMPG. Likewise, the linewidth in both the proton and nitrogen dimensions were significantly smaller in LMPG (41.6 ± 11.7 and 28.9 ± 6.3 Hz, respectively) than in DPC (87.6 ± 54.9 and 49.4 ± 55.0 Hz, respectively), indicating that peaks are sharper in LMPG. All of these values culminate to a higher signal-to-noise ratio in LMPG (153.3 ± 64.6) than in DPC (15.2 ± 4.2). Taken together, while the TM was folded in both LMPG and DPC, the LMPG sample quality was significantly better in NMR. Thus, LMPG was determined to be the optimal detergent for further solution NMR structural studies of the TM.

4. Conclusion

The LASV TM is an essential part of the GPC, serving as the membrane anchor for GP2 and forming critical interactions with the SSP that are important for the viral lifecycle. The lack of knowledge surrounding

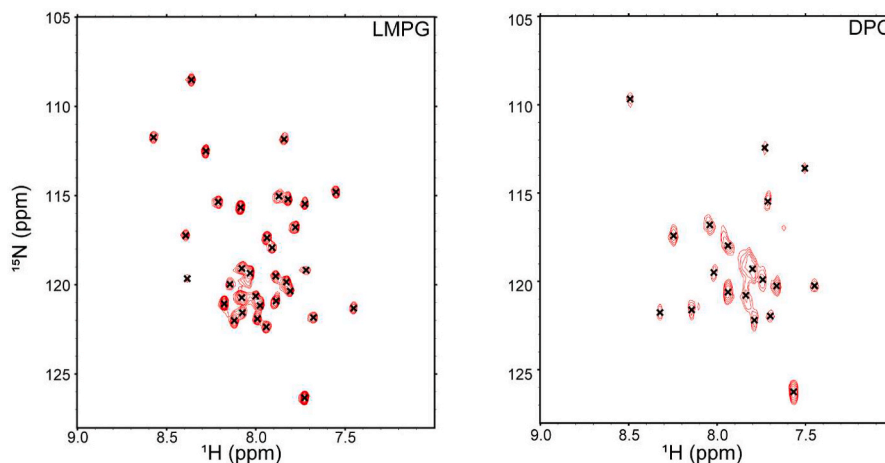


Fig. 6. NMR spectrum of LASV TM. A) ^{15}N - ^1H TROSY-HSQC spectrum of TM in 25 mM Na_2HPO_4 , 100 mM NaCl, 100 mM LMPG or 120 mM DPC, pH 7.0 at 37°C showing well dispersed peaks.

its structure and interactions can partly be attributed to difficulty in purifying it. We have developed a purification protocol that takes advantage of the protein's high propensity to aggregate to assist in purifying the sample. This method was also successfully applied to the larger GP2 construct, showing versatility in the purification method. The characterization in different detergents revealed alpha-helical structure in both LMPG and DPC while LMPG was determined to be the optimal detergent to move forward with structural studies. This work can lead to further biochemical and biophysical studies of the TM to understand its role in the various parts of the LASV lifecycle and has the potential to be applied to other membrane proteins that are difficult to purify.

Author contributions

P.M.K. and J.L. determined the experimental design. P.M.K., H-N.P., S.D.C., performed the research. All authors analyzed data and wrote the paper.

Declaration of competing interest

The authors declare that they have no known competing financial interests or personal relationships that could have appeared to influence the work reported in this paper.

Data availability

Data will be made available on request.

Acknowledgments

We are grateful to the University of Maryland College Park for providing startup funds that allowed us to conduct this research. We would also like to thank undergraduate Joshua Rich, D. Zhang, and Y. Li for their assistance in research, NMR spectroscopy, and mass spectrometry, respectively.

Appendix A. Supplementary data

Supplementary data to this article can be found online at <https://doi.org/10.1016/j.bbrep.2022.101409>.

References

- J.B. McCormick, P.A. Webb, J.W. Krebs, K.M. Johnson, E.S. Smith, A prospective study of the epidemiology and ecology of lassa fever, *J. Infect. Dis.* 155 (1987) 437–444, <https://doi.org/10.1093/infdis/155.3.437>.
- J.K. Richmond, D.J. Baglole, Lassa fever: epidemiology, clinical features, and social consequences, *BMJ* 327 (2003) 1271, <https://doi.org/10.1136/bmj.327.7426.1271>.
- E. Lecompte, E. Fichet-Calvet, S. Daffis, K. Koulémou, O. Sylla, F. Kourouma, A. Doré, B. Soropogui, V. Aniskin, B. Allali, S.K. Kan, A. Lalis, L. Koivogui, S. Günther, C. Denys, J. ter Meulen, *Mastomys natalensis* and 1 Lassa fever, West Africa, *Emerg. Infect. Dis.* 12 (2006) 1971–1974, <https://doi.org/10.3201/eid1212.060812>.
- O.B. Salu, O.S. Amoo, J.O. Shaibu, C. Abejegah, O. Ayodeji, A.Z. Musa, I. Idigbe, O. C. Ezechi, R.A. Audu, B.L. Salako, S.A. Omilabu, Monitoring of Lassa virus (LASV) infection in suspected and confirmed cases in Ondo State, Nigeria, *Pan Afr Medical J* 36 (2020) 253, <https://doi.org/10.11604/pamj.2020.36.253.22104>.
- O. Ogbu, E. Ajuluchukwu, C.J. Uneke, Lassa fever in West African sub-region: an overview, *J Vector Dis* 44 (2007) 1–11.
- A.P. Salam, A. Duvignaud, M. Jaspard, D. Malvy, M. Carroll, J. Tarning, P. L. Olliaro, P.W. Horby, Ribavirin for treating Lassa fever: a systematic review of pre-clinical studies and implications for human dosing, *PLoS Neglected Trop. Dis.* 16 (2022), e0010289, <https://doi.org/10.1371/journal.pntd.0010289>.
- K.A. Eberhardt, J. Mischlinger, S. Jordan, M. Groger, S. Günther, M. Ramharter, Ribavirin for the treatment of Lassa fever: a systematic review and meta-analysis, *Int. J. Infect. Dis.* 87 (2019) 15–20, <https://doi.org/10.1016/j.ijid.2019.07.015>.
- M.S. Mehand, F. Al-Shorbaji, P. Millett, B. Murgue, The WHO R&D Blueprint: 2018 review of emerging infectious diseases requiring urgent research and development efforts, *Antivir. Res.* 159 (2018) 63–67, <https://doi.org/10.1016/j.antiviral.2018.09.009>.
- G.P. Holmes, J.B. McCormick, S.C. Trock, R.A. Chase, S.M. Lewis, C.A. Mason, P. A. Hall, L.S. Brammer, G.I. Perez-Orozco, M.K. McDonnell, J.P. Paulissen, L. B. Schonberger, S.P. Fisher-Hoch, Lassa fever in the United States, *N. Engl. J. Med.* 323 (1990) 1120–1123, <https://doi.org/10.1056/nejm199010183231607>.
- World Health Organization, Disease outbreak news; Lassa fever – United Kingdom of Great Britain and Northern Ireland, 21 February, Available at: <https://www.who.int/emergencies/disease-outbreak-news/item/lassa-fever-united-kingdom-of-great-britain-and-northern-ireland>, 2022.
- H.N. Pennington, J. Lee, Lassa virus glycoprotein complex review: insights into its unique fusion machinery, *Biosci. Rep.* (2022), <https://doi.org/10.1042/bsr20211930>.
- S. Shankar, L.R. Whitby, H.E. Casquilho-Gray, J. York, D.L. Boger, J.H. Nunberg, Small-molecule fusion inhibitors bind the pH-sensing stable signal peptide-GP2 subunit interface of the lassa virus envelope glycoprotein, *J. Virol.* 90 (2016) 6799–6807, <https://doi.org/10.1128/jvi.00597-16>.
- J. Lee, D.A. Nyenhuis, E.A. Nelson, D.S. Cafiso, J.M. White, L.K. Tamm, Structure of the Ebola virus envelope protein MPER/TM domain and its interaction with the fusion loop explains their fusion activity, *Proc. Natl. Acad. Sci. USA* 114 (2017) E7987–E7996, <https://doi.org/10.1073/pnas.1708052114>.
- D.-K. Chang, S.-F. Cheng, E.A.B. Kantchev, C.-H. Lin, Y.-T. Liu, Membrane interaction and structure of the transmembrane domain of influenza hemagglutinin and its fusion peptide complex, *BMC Biol.* 6 (2008) 2, <https://doi.org/10.1186/1741-7007-6-2>.
- B. Hu, H.C. Tina, T. Christoph, V. Michael, Cholesterol binding to the transmembrane region of a group 2 hemagglutinin (HA) of influenza virus is essential for virus replication, affecting both virus assembly and HA fusion activity, *J. Virol.* 93 (2019), <https://doi.org/10.1128/jvi.00555-19>.
- J. Lee, A.J.B. Kreutzberger, L. Odongo, E.A. Nelson, D.A. Nyenhuis, V. Kiessling, B. Liang, D.S. Cafiso, J.M. White, L.K. Tamm, Ebola virus glycoprotein interacts with cholesterol to enhance membrane fusion and cell entry, *Nat. Struct. Mol. Biol.* 28 (2021) 181–189, <https://doi.org/10.1038/s41594-020-00548-4>.
- B. Apellániz, R. Edurne, C. Pablo, R.-I. José, H. Nerea, D. Carmen, J.L. Nieva, Cholesterol-dependent membrane fusion induced by the gp41 membrane-proximal external region–transmembrane domain connection suggests a mechanism for broad HIV-1 neutralization, *J. Virol.* 88 (2014) 13367–13377, <https://doi.org/10.1128/jvi.02151-14>.
- D. Pinto, C. Fenwick, C. Caillat, C. Silacci, S. Guseva, F. Dehez, C. Chipot, S. Barbieri, A. Minola, D. Jarrossay, G.D. Tomaras, X. Shen, A. Riva, M. Tarkowski, O. Schwartz, T. Bruel, J. Dufloo, M.S. Seaman, D.C. Montefiori, A. Lanzavecchia, D. Corti, G. Pantaleo, W. Weissenhorn, Structural basis for broad HIV-1 neutralization by the MPER-specific human broadly neutralizing antibody LN01, *Cell Host Microbe* 26 (2019) 623–637, <https://doi.org/10.1016/j.chom.2019.09.016>, e8.
- G. Zhang, J. Cao, Y. Cai, Y. Liu, Y. Li, P. Wang, J. Guo, X. Jia, M. Zhang, G. Xiao, Y. Guo, W. Wang, Structure-activity relationship optimization for lassa virus fusion inhibitors targeting the transmembrane domain of GP2, *Protein Cell* 10 (2019) 137–142, <https://doi.org/10.1007/s13238-018-0604-x>.
- X. Zhang, K. Tang, Y. Guo, The antifungal isavuconazole inhibits the entry of lassa virus by targeting the stable signal peptide-GP2 subunit interface of lassa virus glycoprotein, *Antivir. Res.* 174 (2020), 104701, <https://doi.org/10.1016/j.antiviral.2019.104701>.
- J.R. Burgeson, D.N. Gharaibeh, A.L. Moore, R.A. Larson, S.M. Amberg, T.C. Bolken, D.E. Hruby, D.C. Dai, Lead optimization of an acylhydrazonone scaffold possessing antiviral activity against Lassa virus, *Bioorg. Med. Chem. Lett* 23 (2013) 5840–5843, <https://doi.org/10.1016/j.bmcl.2013.08.103>.
- C. Diefenderfer, J. Lee, S. Mlyanarski, Y. Guo, K.J. Glover, Reliable expression and purification of highly insoluble transmembrane domains, *Anal. Biochem.* 384 (2009) 274–278, <https://doi.org/10.1016/j.ab.2008.09.038>.
- M. Tang, R. Cao, L. Du, J. Xu, B. Wu, B. Ouyang, Ni²⁺ catalyzed cleavage of TrpLE-fused small transmembrane peptides, *ChemBiochem* 23 (2022), e202100514, <https://doi.org/10.1002/cbic.202100514>.
- D. Wessel, U.I. Flügge, A method for the quantitative recovery of protein in dilute solution in the presence of detergents and lipids, *Anal. Biochem.* 138 (1984) 141–143, [https://doi.org/10.1016/0003-2697\(84\)90782-6](https://doi.org/10.1016/0003-2697(84)90782-6).
- A.J. Miles, S.G. Ramalli, B.A. Wallace, DichroWeb, a website for calculating protein secondary structure from circular dichroism spectroscopic data, *Protein Sci.* 31 (2022) 37–46, <https://doi.org/10.1002/pro.4153>.
- N. Sreerama, R.W. Woody, Estimation of protein secondary structure from circular dichroism spectra: comparison of CONTIN, SELCON, and CDSSTR methods with an expanded reference set, *Anal. Biochem.* 287 (2000) 252–260, <https://doi.org/10.1006/abio.2000.4880>.
- N. Sreerama, S.Yu Venyaminov, R.W. Woody, Estimation of protein secondary structure from circular dichroism spectra: inclusion of denatured proteins with native proteins in the analysis, *Anal. Biochem.* 287 (2000) 243–251, <https://doi.org/10.1006/abio.2000.4879>.
- P. Manavalan, W.C. Johnson, Variable selection method improves the prediction of protein secondary structure from circular dichroism spectra, *Anal. Biochem.* 167 (1987) 76–85, [https://doi.org/10.1016/0003-2697\(87\)90135-7](https://doi.org/10.1016/0003-2697(87)90135-7).
- L.A. Compton, W.C. Johnson, Analysis of protein circular dichroism spectra for secondary structure using a simple matrix multiplication, *Anal. Biochem.* 155 (1986) 155–167, [https://doi.org/10.1016/0003-2697\(86\)90241-1](https://doi.org/10.1016/0003-2697(86)90241-1).
- D. Frank, G. Stephan, V.W. Geerten, Z. Guang, P. John, B. Ad, NMRPipe: a multidimensional spectral processing system based on UNIX pipes, *J. Biomol. NMR* 6 (1995) 277–293, <https://doi.org/10.1007/bf00197809>.
- L. Woonghee, T. Marco, M.L. John, NMRFAM-SPARKY: enhanced software for biomolecular NMR spectroscopy, *Bioinformatics* 31 (2015) 1325–1327, <https://doi.org/10.1093/bioinformatics/btu830>.

- [32] M.W. Maciejewski, A.D. Schuyler, M.R. Gryk, I.I. Moraru, P.R. Romero, E.L. Ulrich, H.R. Eghbalnia, M. Livny, F. Delaglio, J.C. Hoch, NMRbox: a resource for biomolecular NMR computation, *Biophys. J.* 112 (2017) 1529–1534, <https://doi.org/10.1016/j.bpj.2017.03.011>.
- [33] Y. Hatefi, W.G. Hanstein, [77] Destabilization of membranes with chaotropic ions, *Methods Enzymol.* 31 (1974) 770–790, [https://doi.org/10.1016/0076-6879\(74\)31080-4](https://doi.org/10.1016/0076-6879(74)31080-4).
- [34] J.A. Julien, A.L. Pellett, S.S. Shah, N.J. Wittenberg, K.J. Glover, Preparation and characterization of neutrally-buoyant oleosin-rich synthetic lipid droplets, *Biochimica Et Biophysica Acta Bba - Biomembr.* 1863 (2021), 183624, <https://doi.org/10.1016/j.bbamem.2021.183624>.
- [35] E. Hwang, H. Cheong, S. Kim, O. Kwon, K.Y. Blain, S. Choe, K.J. Yeo, Y.W. Jung, Y. H. Jeon, C. Cheong, Crystal structure of the EnvZ periplasmic domain with CHAPS, *FEBS Lett.* 591 (2017) 1419–1428, <https://doi.org/10.1002/1873-3468.12658>.
- [36] R. Puthenveetil, O. Vinogradova, Solution NMR: a powerful tool for structural and functional studies of membrane proteins in reconstituted environments, *J. Biol. Chem.* 294 (2019) 15914–15931, <https://doi.org/10.1074/jbc.rev119.009178>.
- [37] Q. Fu, J.J. Chou, A trimeric hydrophobic zipper mediates the intramembrane assembly of SARS-CoV-2 spike, *J. Am. Chem. Soc.* 143 (2021) 8543–8546, <https://doi.org/10.1021/jacs.1c02394>.
- [38] B. Chen, J.J. Chou, Structure of the transmembrane domain of HIV-1 envelope glycoprotein, *FEBS J.* 284 (2017) 1171–1177, <https://doi.org/10.1111/febs.13954>.
- [39] D.J. Benton, A. Nans, L.J. Calder, J. Turner, U. Neu, Y.P. Lin, E. Ketelaars, N. L. Kallewaard, D. Corti, A. Lanzavecchia, S.J. Gamblin, P.B. Rosenthal, J.J. Skehel, Influenza hemagglutinin membrane anchor, *P Natl Acad Sci Usa* 115 (2018) 10112–10117, <https://doi.org/10.1073/pnas.1810927115>.
- [40] D. Mao, E. Wachter, B.A. Wallace, Folding of the mitochondrial proton adenosine triphosphatase proteolipid channel in phospholipid vesicles, *Biochemistry-Us* 21 (1982) 4960–4968, <https://doi.org/10.1021/bi00263a020>.
- [41] N. Sreerama, S.Y.U. Venyaminov, R.W. Woody, Estimation of the number of α -helical and β -strand segments in proteins using circular dichroism spectroscopy, *Protein Sci.* 8 (1999) 370–380, <https://doi.org/10.1110/ps.8.2.370>.
- [42] S. A. Caroline, R.S. Wayne, E.W. Kevin, NIH Image to ImageJ: 25 years of image analysis, *Nat. Methods* 9 (2012) 671, <https://doi.org/10.1038/nmeth.2089>.